

A MODEL OF INTERNAL GRB SHOCKS

Saša Simić

Faculty of Science, University of Kragujevac, P.O. Box 60, 34000 Kragujevac, Serbia and Montenegro

(Received April 18, 2003)

ABSTRACT. The 'inner engines' of Gamma Ray Bursts (GRBs) are well hidden from direct afterglow observations. However, the variability of GRB light curves at beginning of GRB event can bring us information about the nature of the 'inner engines'. Here, we will present a numerical model which can synthesize light curves in the first phase of GRB. At the beginning we assume that an 'inner engine' creates a lot of small masses shock waves which are spreading isotropically and after short period of time (a couple of seconds) disappearing in the surrounding media. This process causes creation of a massive shock wave which interacts with surrounding media and produces the GRB afterglow. The peaks in the light curve arise in the moment of mutual shocks interaction. We will synthesize them from a given dynamics, by assuming synchrotron radiation mechanism.

1. INTRODUCTION

A quest on the GRB mystery is divided in a several parts. The major features like spatial distribution, afterglow, spectral and light curve, collimation, etc., were all more or less well described in the past decade by sophisticated observations (Bloom et al. 1998; Costa et al. 1997; Groot et al. 1998; Kulkarni et al. 1998; Kulkarni et al., 1999; Harrison et al. 1999; Galama et al. 1999) and theoretical models (Mészáros & Rees, 1997; Vietri 1997; Waxman 1997; Sari, Piran & Narayan 1998; Huang, Dai & Lu 1998a, Huang, Dai, Wei & Lu 1998b, Huang, Dai & Lu 1999). But the biggest challenge of this mysterious event lay in its heart – a central engine, often called the progenitor of GRB. Because of the great optical thickness of expanding material, in the first phase of explosion, structural observations of the progenitor are not possible. All that we can accomplish by observation in the first minute of the GRB is a temporal variability of the light curve. It presents a strong, but short fluctuation of energy output with a typical durability of less then a second, and for us a window to the heart of Gamma-Ray Burst. The numerical simulations (Kobayashi, Piran and Sari, 1997; Ramirez &

Fenimore, 2000) for the first phase of explosion, revealed that the γ -rays light curve replicates temporal activity of 'inner engine'. Here we will use internal model to explain connection between dynamics of inner engine and observed light curve. Like in (Kobayashi, Piran and Sari 1997), we will consider ultra relativistic flow of matter as an array of well defined shells with random Lorentz factors, and name them 'small shocks'. They can collide mutually and produce highly irregular light curve.

The aim of this paper is to give a numerical model of small shocks in the first phase, and to synthesize observed light curve.

2. SMALL SHOCKS MODEL

In order to explain a temporal variability of the light curve we propose the following scenario. In the first phase of explosion a central engine creates a great number of small mass highly collimated shocks which spread in all directions. These shocks have high Lorentz factors with different magnitudes, so the faster shocks can catch the slower ones – this is known as the internal model (Kobayashi, Piran & Sari 1997; Fenimore & Ramirez-Ruiz 1999; Piran 2000). When this happens a number of radiating particles sharply increase, to create a pulse in the light curve. Duration of the pulse depends on a width of shocks and on its Lorentz factors, with typical values less than 1s. Because the mass of shocks is relatively low, they have short lives and disappear in a surrounding media shortly after the creation. But the central engine creates them repeatedly in the initial phase. They accelerate particles of the inter-stellar medium (hereafter ISM) around the GRB center, and together create one bigger, more massive shock, which continues to spread. Then starts the second phase of GRB, with creation of the afterglow.

Let us now consider a moving, highly collimated shell, assumed to be part of a sphere. The shell front area is given by $2\pi R^2(1-\cos\theta)$, while its width is R/Γ^2 , according to Blandford and McKee (1976). Therefore the mass of the shell is given by $m_s = 2\pi n m_p (1-\cos\theta) R^3 / \Gamma^2$, where n is a volume density of the shell, θ angle of collimation, m_p is the proton mass, while R designates distance from the center of GRB and Γ shell Lorentz factor. We assume that the volume density of the shell n , is connected with a number density of ISM n_0 , as $n = n_0(4\Gamma + 3)$, (Blandford & McKee, 1976). If the ISM is not

homogenous, then the equation for density must contain another term to take this fact into account. Its full form is then as follows:

$$n = n_0 \left(\frac{R_0}{R} \right)^s (4\Gamma + 3) \quad (1)$$

where s is a constant whose value is 0 in a homogenous case, or 2 for the wind environment, and R_0 is initial value for R . We took over the equations for R and Γ from (Huang, Gou, Dai, Lu, 2000) their equations 3 and 8. Therefore the complete system of differential equations we used, is:

$$\frac{dR}{dt} = c\sqrt{\Gamma^2 - 1} \left[\Gamma + \sqrt{\Gamma^2 - 1} \right], \quad (2)$$

$$\frac{d\Gamma}{dm_s} = -\frac{\Gamma^2 - 1}{M_{ej} + 2(1 - \varepsilon)\Gamma m_s + \varepsilon m_s}, \quad (3)$$

$$\frac{dm_s}{dt} = 2\pi n m_p (1 - \cos \theta) \frac{R^2}{\Gamma^3} \left(3\Gamma \frac{dR}{dt} - 2R \frac{d\Gamma}{dt} \right), \quad (4)$$

where the parameter ε varies from 0, which is an adiabatic, up to 1, to describe a fully radiative expansion, and we take M_{ej} to be the mass of a primary ejected material. Equations (2) to (4) are derived for observer reference frame, and they need to be simultaneously solved, together with the density equation. Initial values of parameters and variables are highly dependent on specific shocks. Here we give some equations and parameter values that will be used. The initial mass of the shock wave $m_{s0} = M_{ej}/\Gamma_0 + 2\pi n_0 m_p (4\Gamma_0 + 3)(1 - \cos \theta_0) R_0^3/\Gamma_0^2$, consist mass of the ejected material M_{ej} and mass of the particles of ISM in the initial volume of the shock. We choose M_{ej} to be $\approx 10^{23}$ gr. which is 5 orders of magnitude less than a mass of the afterglow shock wave (Huang, Dai, Lu, 1999). θ_0 is the initial value for the opening angle of collimation and should be set to values between 0.1 and 0.3 rad. The initial values for Lorentz factor vary from 100 to 1000, and starting diameter is $R_0 = 10^{13} - 5 \cdot 10^{13}$ cm.

If the shock wave on his way out, encounter another, slower one, this event will increase the number of radiating particles. Mathematically, we can model this density disturbance with a gaussian pulse, where the width on the half maximum represents the width of the slower shock, while its height represents its intensity. Using the parameters a and b we can modify the profile of this pulse so that a determine its intensity and b its width. Equation (1) will then have the following form:

$$n = n_0 \left(\frac{R_0}{R} \right)^s (4\Gamma + 3) \left(1 + a \cdot \exp \left[- \left(\frac{R - R_c}{b} \right)^2 \right] \right) \quad (5)$$

where R_c is a position of the shock encounter. If we accept that an average duration of the observed light-curve pulse is less than 1s, then the width of density irregularities is $\approx 10^{12}$ cm, and a position of the shock encounter is $\approx 10^{14}$ cm (see Piran, 2000).

Let us briefly emphasize the physical picture of this scenario. Namely, as we mentioned above, the number of small shocks is created by the central engine. They have collided with each other and created pulses, but if some of shocks do not collide, it will create a background radiation. If a collision is not so intensive - low density shocks - pulses will be very small or will not be created at all. However, if a density of the slower shock is high enough, the faster shock will be stopped. This creates, most intense pulses, and present main mechanism to explain high variability of the light curve.

Emission mechanism of shock waves is based on the synchrotron radiation. We use formula given by Rybicki & Lightman (1979) to calculate it:

$$P'(v') = \frac{\sqrt{3}e^3 B' \gamma_{e\max}}{m_e c^2} \int_{\gamma_{e\min}}^{\gamma_{e\max}} \left(\frac{dN_e'}{d\gamma_e} \right) F \left(\frac{v'}{v_c'} \right) d\gamma_e \quad (6)$$

where e is the electron charge, $dN_e'/d\gamma_e$ is a distribution of radiating electrons in a shock

wave, $v_c' = \frac{3eB'\gamma_e^2}{4\pi m_e c}$ critical frequency, and $B', \gamma_{e\min}, \gamma_{e\max}$ are the magnetic field, minimal and

maximal electron Lorentz factors, respectively given by the equations:

$$B' = \sqrt{8\pi \xi_b^2 n_0 \Gamma m_p c^2 (4\Gamma + 3) \left(\frac{R_0}{R} \right)^s \left(1 + (4\Gamma_c + 3) e^{-\left(\frac{R-R_c}{b} \right)^2} \right)}, \quad (7)$$

$$\gamma_{e\min} = \xi_e \Gamma \frac{m_p}{m_e} \frac{p-1}{p}, \quad \gamma_{e\max} = \frac{10^8}{\sqrt{B'}}.$$

The magnetic field is calculated in a standard way by taking into account that the energy of the this field is a part of total energy of the shock wave, defined by a factor ξ_b whose values

are of the order $\xi_b \approx 0.1$. The function F in equation (6) is of the form $F(x) = x \int_x^\infty K_{5/3}(u) du$,

where $K_{5/3}(u)$ is a second order Bessel function. Usually, the distribution of the electrons in a shock wave is assumed to be a power law function of the electron energy, $dN_e'/d\gamma_e \propto \gamma_e^{-p}$.

However, there is a critical energy above which the synchrotron radiation becomes

significant. This energy is defined by the critical Lorentz factor $\gamma_c = \frac{6\pi m_e c^2 \Gamma^2}{\sigma_T B^2 R}$, which is here derived for a case of thin shell. In our model, an electron distribution is given by (Dai, Huang & Lu, 1999; Huang, Dai, Wei, Lu, 1998b):

i) For $\gamma_c \leq \gamma_{e\min}$,

$$\frac{dN'_e}{d\gamma_e} \propto \gamma_e^{-(p+1)}, \quad (\gamma_{e\min} \leq \gamma_e \leq \gamma_{e\max}); \quad (8)$$

ii) For $\gamma_{e\min} \leq \gamma_c \leq \gamma_{e\max}$,

$$\frac{dN'_e}{d\gamma_e} \propto \begin{cases} \gamma_e^{-p}, & (\gamma_{e\min} \leq \gamma_e \leq \gamma_c), \\ \gamma_e^{-(p+1)}, & (\gamma_c \leq \gamma_e \leq \gamma_{e\max}) \end{cases}; \quad (9)$$

iii) For $\gamma_c > \gamma_{e\max}$,

$$\frac{dN'_e}{d\gamma_e} \propto \gamma_e^{-p}, \quad (\gamma_{e\min} \leq \gamma_e \leq \gamma_{e\max}). \quad (10)$$

If we assume that D_L is a luminosity distance and Θ angle closed by velocity vector and the observation line, with $\mu = \cos\Theta$, then the observed flux can be calculate according to (Huang, Gou, Dai, Lu, 2000):

$$S_\nu = \frac{1}{\Gamma^3 (1 - \beta\mu)^3} \frac{1}{4\pi D_L^2} P'(\Gamma(1 - \beta\mu)\nu), \quad (11)$$

where all primed variables are defined in the co-moving frame.

3. RESULTS AND DISCUSSION

Let us consider a main shock wave on its way out from the GRB center, with some initial values of Lorentz factor and distance, $\Gamma_0 = 200$ and $R_0 = 5 \cdot 10^{13} \text{ cm}$. Now, we can calculate initial mass of the shock based on equation in chapter 2. with the result $m_{s0} \approx 2.0 \cdot 10^{20} \text{ gr}$. The motion of a shock wave will cause the synchrotron radiation, which will produce a continuous background flux. But when this shock encounters another, the slower one, a pulse discontinuity will be created. Because of small mass of these shocks, their lifetimes will be shortened and their Lorentz factor will drop rapidly. We will set up a parameter b in order to get a width of the slower shock to the order of $\approx 2.0 \cdot 10^{12} \text{ cm}$. The

parameters which are used to calculate the flux have standard values: $\xi_e = 0.1$, $\xi_b^2 = 0.01$, $p = 2.5$, $\Theta = 0$, $D_L \approx 10^{29} \text{ cm}$. The parameters ξ and s can be changed in order to observe a radiational or the adiabatic case and the homogenous case as related to the wind environment. Initially, we can take that an ejected mass, $M_{ej} \approx 5 \cdot 10^{22} \text{ gr.}$, and that the number density of ISM is $n = 10^6 \text{ cm}^{-3}$. The present value M_{ej} is taken to fit some of the usual observation.

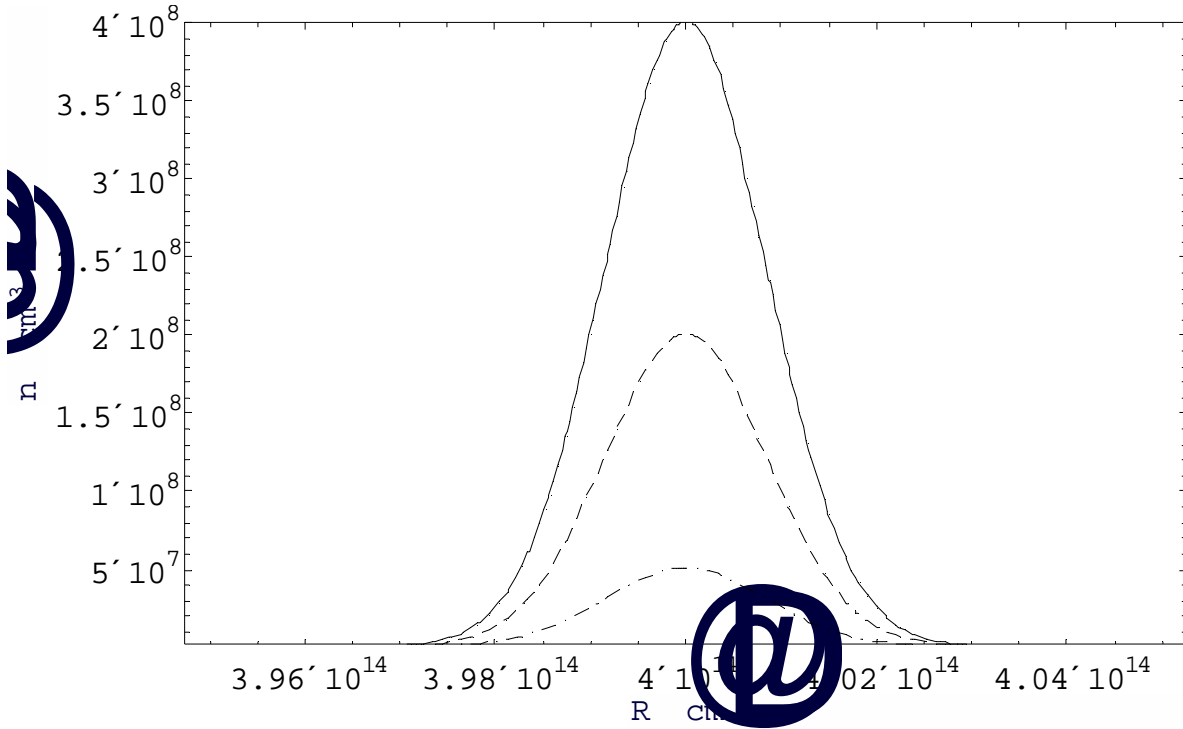


Fig. 2. Shape of the ISM density peak for the moving shock. Three lines presents different values for parameter a . ($a = 400$ – full line; $a = 200$ – dashed line; $a = 50$ – dash/dotted line)

Now let us suppose that at the distance R_c our shock wave interacts with another one, what will a cause pulse in density of ISM for the faster shock. We take that this pulse has a form shown in Fig. 2. Changing the parameters a and b we can setup a height of the pulse and its width, and further its density and width of the slower shock. The parameter a can be interpreted as $a = 4\Gamma_c + 2$, and connected with the equation for the shock width, what yields $\Delta = 16R_c / (a - 2)^2 \approx 10^{12} \text{ cm}$, where Γ_c is the Lorentz factor of slower shock. Now if we make calculation, the results can be presented graphically as in Fig. 3.

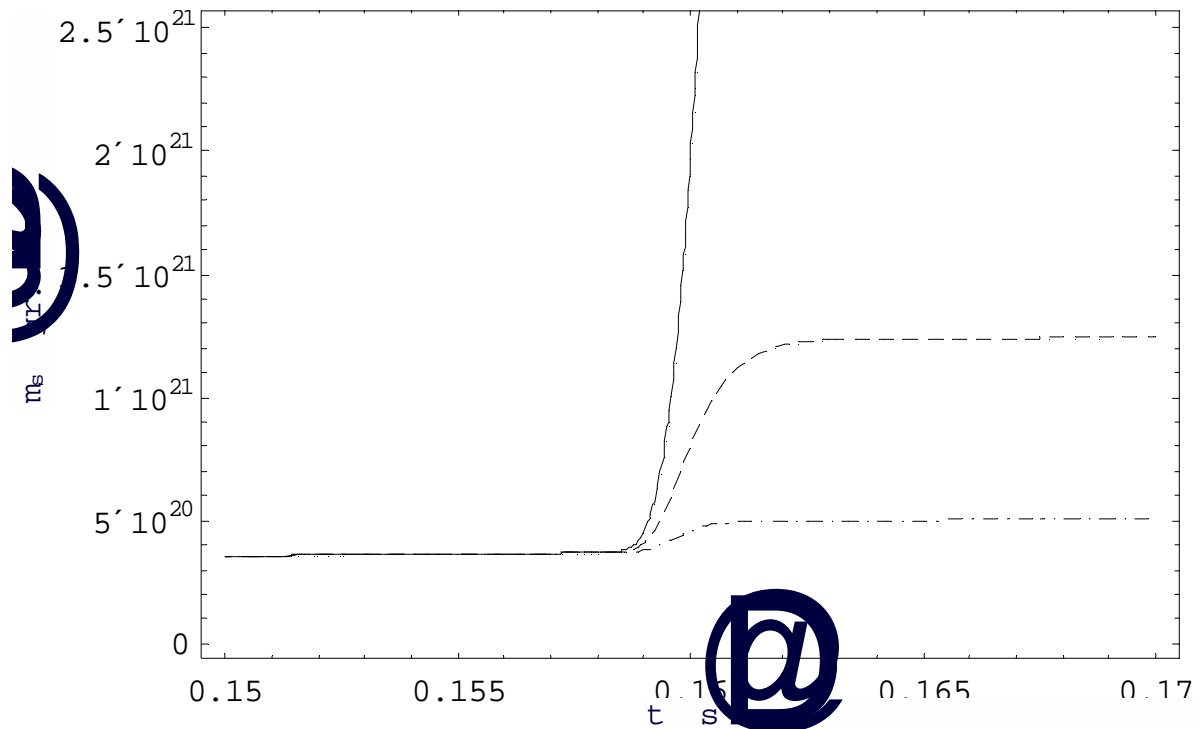


Fig. 3. Evolution of main shock mass. Three lines presents different values for parameter a .

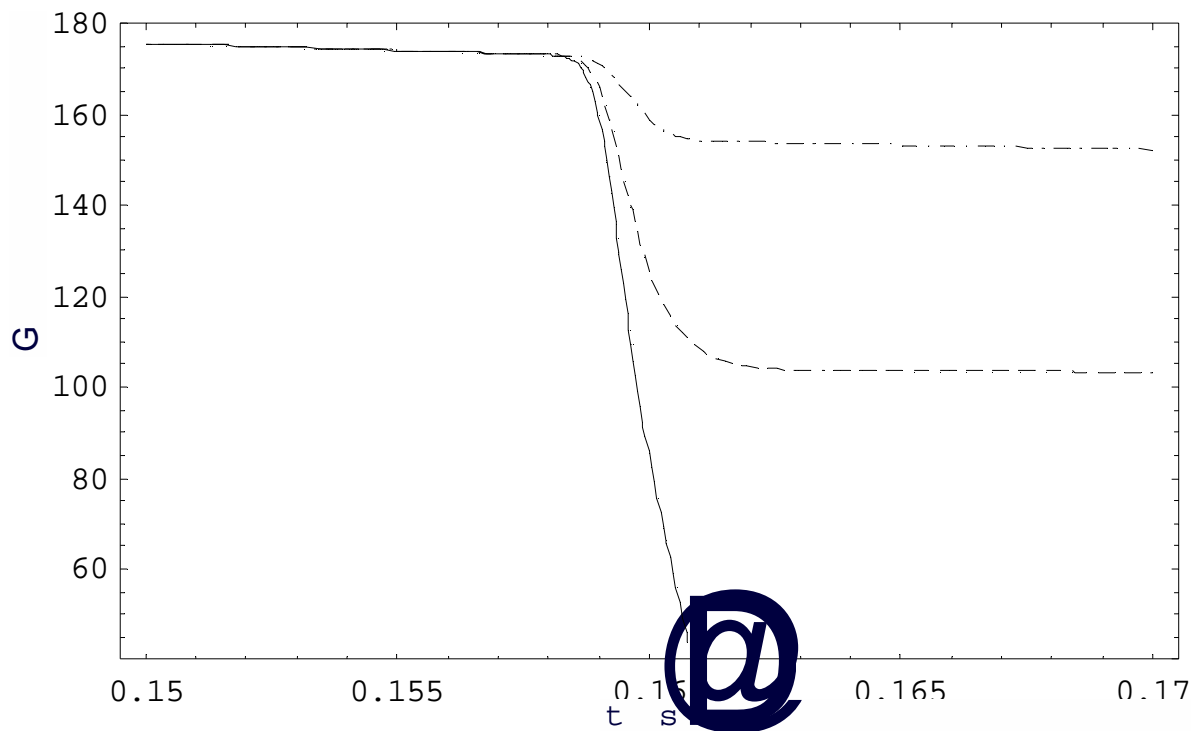


Fig. 4. Evolution of main shock Lorentz factor. Three lines presents different values for parameter a .

We see that at the moment of interaction the mass of the main shock sharply increases for an amount, which depends on density and width of the slower one. On the contrary, its Lorentz factor then sharply decreases. In a Fig. 3. we see the evolution of mass for three different values of the parameter a . We expect that for a denser slower shock we obtain higher

mass increase, what will cause rapid slowing down of the main shock (Fig. 4). This will strongly influence the radiated energy and consequently the height of the light curve peak. The moment of interaction measured in a reference frame of the main shock, can also change the intensity of peaks, and causes more radiated energy, if the interaction happened earlier whether then later when the main shock is slower.

It is important to notice that if the density and width of the slower shock are big enough, the main shock will be stopped, Fig. 3. and 4. full line. This produces the highest peaks in the light curve. One can put a question as to whether this breaking of charged particles can cause radiation not by a synchrotron mechanism but rather by a *bremstrahlung* effect. This could be important if a breaking of main shock is rapid, which is the case when parameters a and b are big enough.

Now let us present a peak of the light curve synthesized from the main shock wave. It is shown for different values of parameters a and b in Fig. 5. As we can see the most intense radiation is coming when moving shock is stopped. A further increase of parameter a can not increase a peak of the light curve, but can produce its steeper deceleration. Consequently, that may cause a significant *bremstrahlung* radiation. However, importance of these phenomena will be subject of another scientific study.

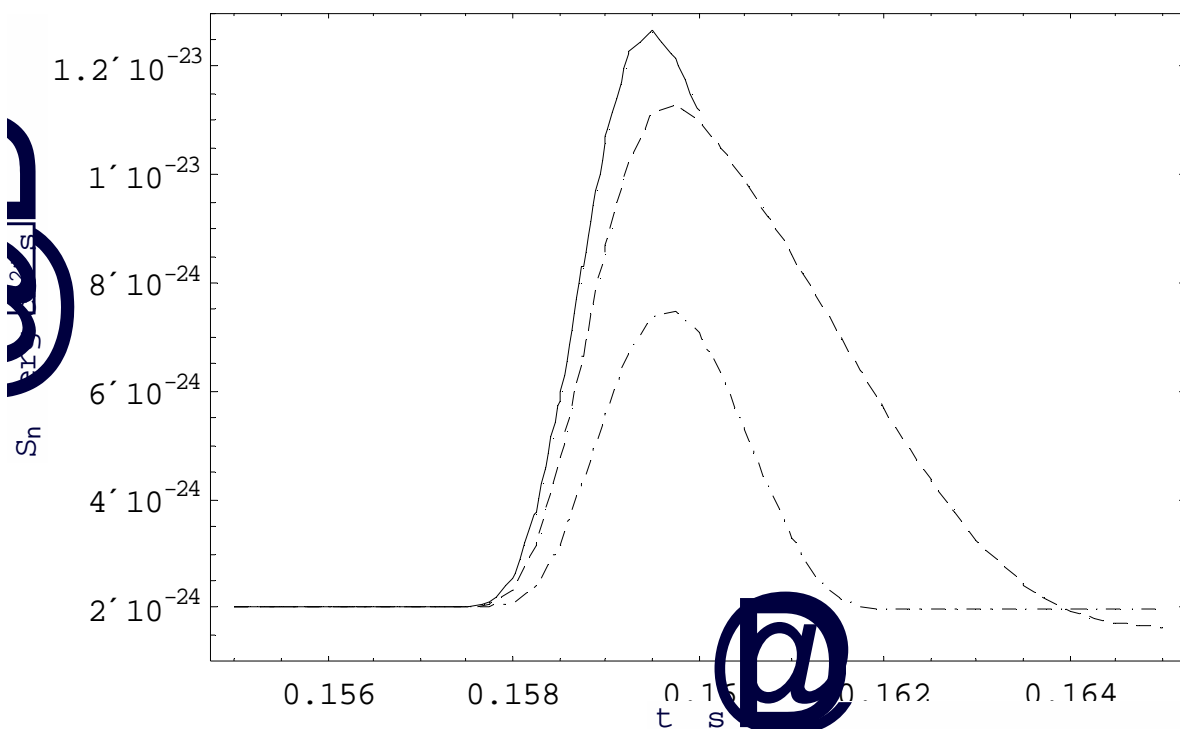


Fig. 5. Synthesized pulse of light curve. Three lines presents different values for parameter a .

ACKNOWLEDGMENTS

This work was supported by the Ministry of Science, Technologies and Development of Serbia through the project 'Astrophysical Spectroscopy of Extragalactic Objects'.

References

- [1] Blandford, R.D. and McKee, C.F., 1976, *Physics of Fluids*, 19, 1130
- [2] Bloom, J.S., Frail, D.A. Kulkarni, S.R. Djorgovski, S.G. Halpern, J.P. Marzke, R.O. Patton, D.R. Oke, J.B. Horne, K.D. Gomer, R. Goodrich, R. Campbell, R. Moriarty-Schieven, G.H. Redman, R.O. Feldman, P. A. Costa, E. Masetti, N. et al., 1998, *ApJ*, 508, L21
- [3] Costa, E. Frontera, F. Heise, J. Feroci, M. in 't Zand, J. Fiore, F. Cinti, M. N. dal Fiume, D. Nicastro, L. Orlandini, M. Palazzi, E. Rapisarda, M. Zavattini, G. Jager, R. Parmar, A. Owens, A. Molendi, S. Cusumano, G. Maccarone, M. C. Giarrusso, S. Coletta, A. Antonelli, L. A. Giommi, P. Muller, J. M. Piro, L. Butler, R. C., 1997, *Nature*, 387, 783
- [4] Dai, Z.G., Huang, Y.F., Lu, T., 1999, *ApJ*, 520, 634
- [5] Fenimore, E.E., Ramirez-Ruiz, E., 1999, astro-ph/9909299
- [6] Galama, T. J. Briggs, M. S. Wijers, R. A. M. Vreeswijk, P. M. Rol, E. Band, D. van Paradijs, J. Kouveliotou, C. Preece, R. D. Bremer, M. Smith, I. A. Tilanus, R. P. J. de Bruyn, A. G. Strom, R. G. Pooley, G. Castro-Tirado, A. J. Tanvir, N. Robinson, C. Hurley, K. Heise, J. Telting, J. Rutten, R. G. M. Packham, C. Swaters, R. Davies, J. K. Fassia, A. Green, S. F. Foster, M. J. Sagar, R. Pandey, A. K. Nilakshi Yadav, R. K. S. Ofek, E. O. Leibowitz, E. Ibbetson, P. Rhoads, J. Falco, E. Petry, C. Impey, C. Geballe, T. R. Bhattacharya, D. 1999, *Nature*, 398, 394
- [7] Groot, P. J. Galama, T. J. Vreeswijk, P. M. Wijers, R. A. M. J. Pian, E. Palazzi, E. van Paradijs, J. Kouveliotou, C. in 't Zand, J. J. M. Heise, J. Robinson, C. Tanvir, N. Lidman, C. Tinney, C. Keane, M. Briggs, M. Hurley, K. Gonzalez, J.-F. Hall, P. Smith, M. G. Covarrubias, R. Jonker, P. Casares, J. Frontera, F. Feroci, M. Piro, L. Costa, E. Smith, R. Jones, B. Windridge, D. Bland-Hawthorn, J. Veilleux, S. Garcia, M. Brown, W. R. Stanek, K. Z. Castro-Tirado, A. J. Gorosabel, J. Greiner, J. Jaeger, K. Bohm, A. B. Fricke, K. J., 1998, *ApJ*, 502, L123
- [8] Harrison, F. A. Bloom, J. S. Frail, D. A. Sari, R. Kulkarni, S. R. Djorgovski, S. G. Axelrod, T. Mould, J. Schmidt, B. P. Wieringa, M. H. Wark, R. M. Subrahmanyam, R. McConnell, D. McCarthy, P. J. Schaefer, B. E. McMahon, R. G. Markze, R. O. Firth, E. Soffitta, P. Amati, L., 1999, *ApJ*, 523, L121
- [9] Huang, Y. F., Dai, Z. G., Lu, T., 1999, *MNRAS*, 309, 513
- [10] Huang, Y.F., Dai, Z.G., Lu, T., 1998a, *A&A*, 336, L69
- [11] Huang, Y.F., Dai, Z.G., Wei, D.M., Lu, T., 1998b, *MNRAS*, 298, 459

- [12] Huang, Y.F., Gou, L.J., Dai, Z.G., Lu, T., 2000, ApJ, 543, 90H
- [13] Kobayashi, S., Piran, T., & Sari, R., 1997, ApJ, 490, 92
- [14] Kulkarni, S. R. Djorgoski, S. G. Ramaprakash, A. N. Goodrich, R. Bloom, J. S. Adelberger, K. L. Kundic, T. Lubin, L. Frail, D. A. Frontera, F. Feroci, M. Nicastro, L. Barth, A. J. Davis, M. Filippenko, A. V. Newman, J. et al., 1998, Nature, 393, 35
- [15] Kulkarni, S. R. Djorgovski, S. G. Odewahn, S. C. Bloom, J. S. Gal, R. R. Koresko, C. D. Harrison, F. A. Lubin, L. M. Armus, L. Sari, R. Illingworth, G. D. Kelson, D. D. Magee, D. K. van Dokkum, P. G. Frail, D. A. Mulchaey, J. S. Malkan, M. A. McClean, I. S. Teplitz, H. I. Koerner, D. Kirkpatrick, D. Kobayashi, N. Yadigaroglu, I.-A. Halpern, J. Piran, T. Goodrich, R. W. Chaffee, F. H. Feroci, M. Costa, E. et al., 1999, Nature, 398, 389
- [16] Mészáros, P., Rees, M. J., 1997, ApJ, 476, 232
- [17] Piran, T., 2000, Phys. Report, 333, 529
- [18] Ramirez-Ruiz, E., Fenimore, E. E., 2000, ApJ, 539, 712
- [19] Rybicki, G.B., Lightman, A.P., 1979, *Radiative Processes in Astrophysics*, Wiley, New York
- [20] Sari, R., Piran, T., Narayan, R., 1998, ApJ, 497, L17
- [21] Vietri, M., 1997, ApJ, 488, L105
- [22] Waxman, E., 1997, ApJ, 485, L5